Contents lists available at GrowingScience

Engineering Solid Mechanics

homepage: www.GrowingScience.com/esm

Effects of cold joints on the structural behaviour of polyurethane rigid foam panels

Saeed Nemati[a*], Pezhman Sharafi[a] and Bijan Samali[a]

[a]*Centre for Infrastructure Engineering, Western Sydney University, Australia*

ARTICLEINFO

Article history:
Received 10 October, 2018
Accepted 23 December 2018
Available online
23 December 2018

Keywords:
Foam
Panel
Seam
Tensile strength
Cyclic loading

ABSTRACT

Foam made panels as efficient building elements are becoming a major role player in modular construction with a variety of applications worldwide. However, construction accuracy, technology, and method can have serious effects on the panels' behavior. In this study, using a unique pneumatic pressure testing rig, bending tests are conducted on the two types of rigid polyurethane panels. The panels are categorized based on the existence of construction cold joints (seams) as S (Seamless) type and TS (Transverse Seams) type. The S type panels are tested under monotonic uniform loading with a maximum nominal pressure of about 1 atm as the witness specimens. The TS panels are tested under both monotonic and cyclic uniform loading, and the deflections-pressure behavior obtained. The results show that S panels could resist up to 0.77 atm under monotonic uniform loading, while the minimum tensile strength of the foam is 13 MPa. In addition, panels with transverse seams collapsed under monotonic and cyclic loads at an average of 0.46 atm and 0.33 atm respectively but at the same position, located on the seamed section, which represent the same failure mode. Based on the results, the seamed section exhibited a maximum tensile strength of about 33.1% of an intact section under monotonic loading; and 27.9% lower results under cyclic loading.

1. Introduction

Lightweight structural panels are important mobile and quickly assembled structures. These types of panels are a form of modular construction, implemented in residential buildings and industrial structures (Sharafi et al., 2017). Some advantages of this system are: (1) They can sit on each other as plate, so substantially reduce the transportation cost per unit; (2) they can be made in any sizes and consequently cut the construction time; (3) they can be connected to each other quickly for quick assembly construction and (4) they can play the role of structural elements, partitions and/or insulators at the same time.

Such advantages make structural panels an attractive alternative to the traditional construction systems in the recent years. Wide ranges of these panels are made from new lightweight components such as foams. Many types of foams are on the market and the Polyurethane (PU) foams are the most popular types (Defonseka, 2013). The lightweight penalized foam made products are popular because they are light, easy to install and have good thermal and acoustic properties. However, the effects of construction accuracy, technology and methods on the mechanical behaviour of structural panels are

* Corresponding author.
E-mail addresses: S.Nemati@uws.edu.au (S. Nemati)

doi: 10.5267/j.esm.2018.12.003

significant as similar as other infrastructures. One of the most important construction problems of foam made panels is cold joints, which is also known as seams. When the placing of foam in the panels is delayed or interrupted for some reasons, the foam that has already been placed starts to condense, producing a kind of construction joint (seam) called a cold joint between it and newly placed foam. Seam is a plane under mixed material, or a fold that is developed within the rising foam mass, which appears as a line on the foam surface or section, as shown in Fig. 1 (ASTM-E1730, 2015). Such joints between new and old portions of foam that are formed when new foam is placed adjacent to the foam that has hardened or has started to harden, may have negative effects on the strength of rigid foam panel. Hence, attention must be paid to the position and direction of the joints, and the effects on the structural behaviour.

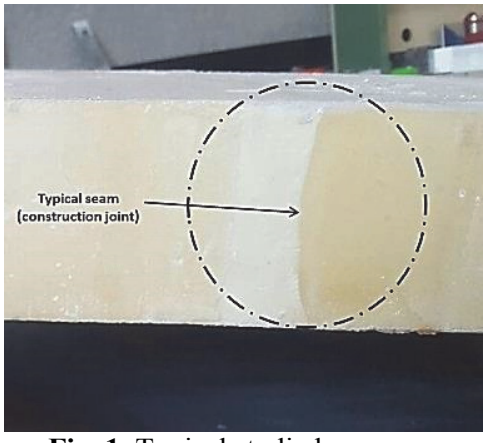

Fig. 1. Typical studied seams

There are some research studies on the structural applications of foams. Zenkert and Burman (2009) studied tension, compression and shear fatigue of a closed cell polymer foam, where the foam is tested quasistatically in tension, compression and shear. Fatigue crack propagation in a closed-cell foam is experimentally investigated by some researchers (Fan et al., 2017). They conducted series of fatigue tests to obtain crack length vs loading cycle number and fatigue crack propagation rate vs stress intensity. In a similar work, researchers (Zhao et al., 2015) carried out tension–tension fatigue tests to investigate the fatigue of closed-cell foam. Noble and Lilley (1981) studied the fatigue crack growth in rigid polyurethane foam under conditions of constant load-amplitude cycling. Shipsha et al. (2000) carried out an experimental study of fatigue crack propagation in polymeric cellular foam cores for sandwich structures. In a similar work, Poapongsakorn and Kanchanomai (2013) investigated the applicability of linear-elastic fracture mechanics, elastic–plastic fracture mechanics and time-dependent fracture mechanics parameter to characterise fatigue crack growth rate of closed-cell polyvinyl chloride. Other researchers performed some dynamic mechanical analyses and flexural fatigue of PVC foams of densities in the range from 75 to 300 kg/m^3 (Kanny et al., 2002), in which the fatigue behaviour was found to be similar to structural materials with a fatigue strength that increased with foam density. Huang and Lin (1996) analysed the fatigue of cellular materials using dimensional arguments. They found out that the fatigue of cellular materials depends on the cyclic stress intensity range, cell size, relative density and the fatigue parameters of used material. Other scientists focused on the influence of pores on crack initiation in monotonic and cyclic tensile loadings (Wang et al., 2016). Pores were shown to have an important influence on strain localization zones for crack initiation both in monotonic tensile and cyclic loadings. Since the crack growth and brittle fracture is a major mode in foam materials subjected to tensile type loads some researchers have studied the fracture toughness and fracture behaviour of such materials (Marsavina et al., 2013; Aliha et al., 2018a,b). Toubia and Elmushyakhi (2017) studied the effects of core joints in sandwich composites under in-plane static and fatigue loads. Their research confirmed that despite the face sheets' primary in-plane load carrying mechanisms, core junction substantially influence the axial fatigue life of the structure.

In this paper, the effect of seams on the structural behaviour of PU rigid foam panels will be studied

through some experiments on the seamed and seamless samples, under monotonic and cyclic loads. The results will be compared with each other in order to investigate the impact of presence of seams on the bending strength of samples.

2. Material properties

To evaluate the basic material properties, in addition to using the manufacturers' data, some experimental tests were carried out. In this regard, PU high-density rigid foam with the density of 192 kg/m^3 was chosen. Table 1 shows the used foam's manufacturing and mechanical properties, provided by the manufacturer and validated in the laboratory using the ASTM 1730 standard specification for rigid foam (ASTM-E1730, 2015). Three 50mm×50mm×50mm cubic specimens were tested by a uniaxial load machine, at a loading rate of 5 mm/min in order to identify the structural properties of the rigid PU foam. The results show that this type of PU foam, which is made of a 100:110 weight ratio mixture of AUSTHANE POLYOL AUW763 and AUSTHANE MDI ISOCYANATE (Fig. 2), can undertake considerable deformation before the failure. In addition, the elastic modulus of foam has been calculated as 135.5 MPa (Nemati et al., 2018; Sharafi et al., 2018a,b).

Table 1. Mechanical and manufacturing properties of the selected PU rigid foam

Mechanical Properties of the PU foam			
Density (kg/m^3)	Compressive yield strength (MPa)	Tensile yield strength (MPa)	Shear yield strength (MPa)
192	3.51	1.896	1.034
Manufacturing Properties			
Cream time[1]	Gel time[2]	Tack free time[3]	
35-40 sec	94 ± 4 sec	115 ± 5 sec	

[1]A measure of the beginning of the foam reaction. Usually characterized by a change in the liquids colour as it begins to rise.
[2]The time when the foam has developed enough gel strength to be dimensionally stable.
[3]The time between the beginning of the foam pour and the point at which the outer skin of the foam loses its stickiness.

3. Description of specimens and test setup

In this study, three series of bending tests were carried out on two types of panelised specimens. Two types of 1500×1000×100 mm^3 rigid polyurethane panels were used: Type S (seamless) and type TS (with transverse seams) specimens. The expansion rate of this type of foam is 3.0, and the average weight of both types of panels is 29.0 kg. In order to make seamless samples, "one shot pouring system" was employed. To that end, 50 litres of mix liquid material is casted in the wooden formworks with a filling rate of 1.25 litres per second. The TS panels were casted with five cold joints H1 to H5, as shown in Fig. 2. In fact, TS specimens were made during six pouring steps, using 8.3 litres of mix liquid material for each step and with the same filling rate. Fig. 3 illustrates the casting schedule for each step.

Fig. 2. transverse seams (H1-H5)Locations of

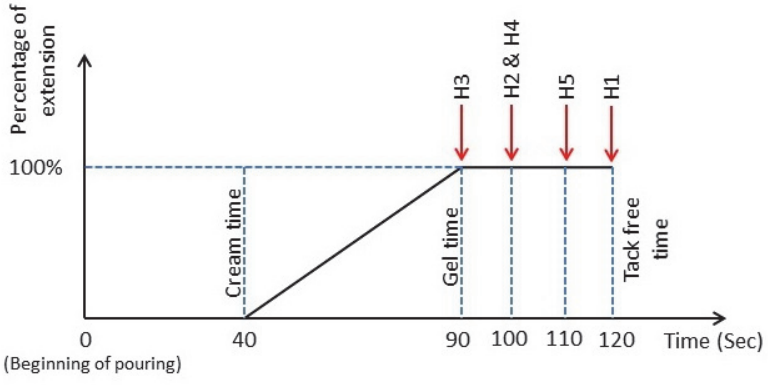

Fig. 3. Casting schedule of seams at TS specimens

3.1 Test Setup

The tests were undertaken using an automated vacuum rig at the Centre for Infrastructure Engineering (CIE) at Western Sydney University. The rig allows for undertaking loading test on panels of heights up to 6m under a vacuum suction of up to 10 kPa. The panels were horizontally loaded into the test chamber, fixed and sealed; the chamber is pulled up by an electric winch until it stands vertically before the suction is applied. The loading regime can be change according to the requirements. In order to adhere to an appropriate regime of loading, the rig enjoys a fully automatic controller, which utilises powerful software developed within the LabView environment (NI, 2016). Fig. 4 shows the vacuum test rig setup, and Fig. 5 illustrates the locations of automatic electrical potentiometers.

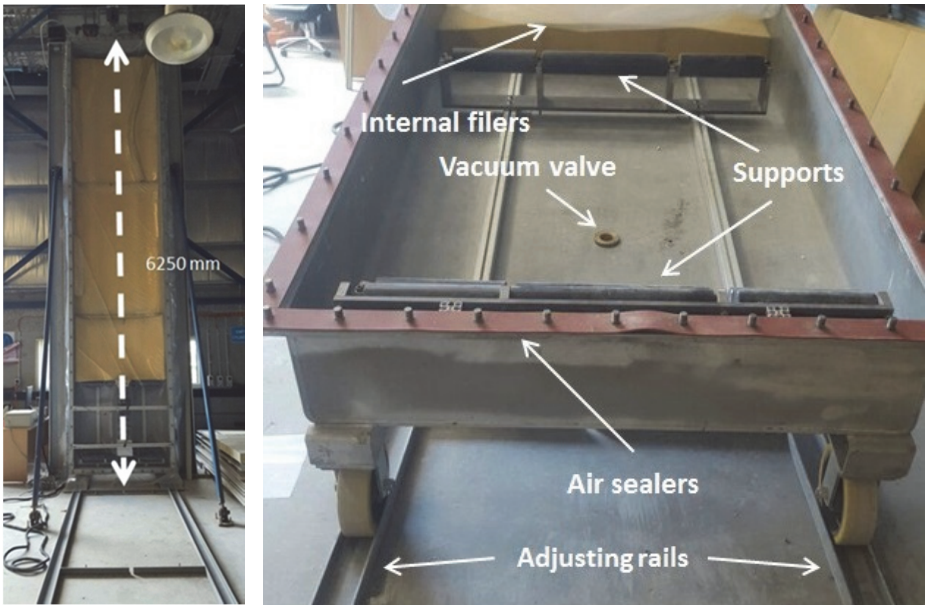

Fig. 4. Details of vacuum testing rig

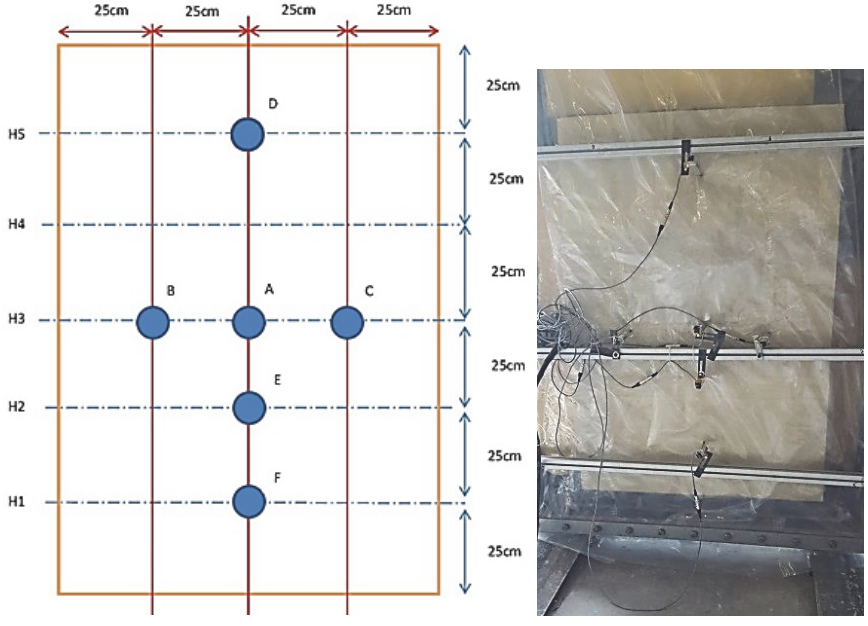

Fig. 5. Arrangement of potentiometers on panels (for all tests)

3.2 Testing Program

Three monotonic tests were conducted on the S and TS specimens, together with three cyclic tests on the TS specimens. Table 2 shows the summary of the test arrangement. First series of bending tests carried out on the S panels using a uniform monotonic under about 1 atm air pressure (Load Regime #1) with a rate of 0.1 atm/min. The second series of bending tests were carried out on the TS panels using the same loading regime (Load Regime #1).The third series of bending tests were conducted on the TS panels, using a predicted cyclic air pressure (Load Regime #2) with a rate of 0.1 atm/min, as shown in Fig. 6.

Table 2. Test arrangement matrix

Test series	Specimen	Number of specimens	Load configuration
1	S	3	Monotonic
2	TS	3	Monotonic
3	TS	3	Cyclic

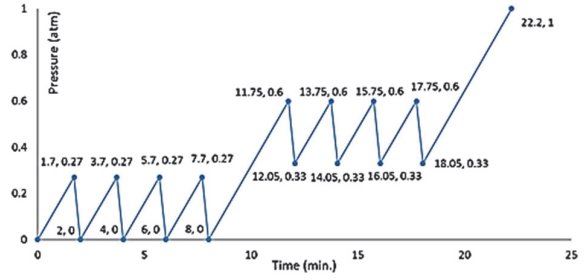

Fig. 6. Cyclic regime of loading, used at second series of bending tests

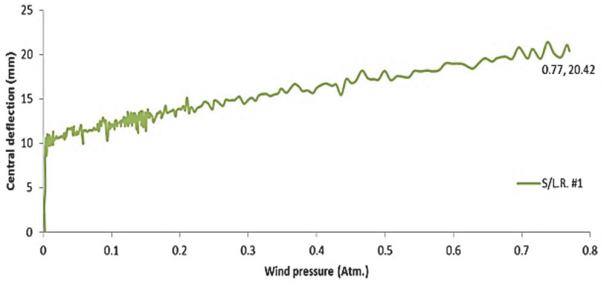

Fig. 7. Vacuum pressure vs average central deflection (point A) for test series #1

4. Test results

For the test series #1, all three seamless panels resisted a maximum of 0.77 atm. Fig.7 and Table 2 show the pressure-deflection diagram and the deflections measured by potentiometer, respectively. Up to a pressure of about 0.23 atm, where shows a large primary deflection, the system is in the adjusting phase, and the pressure is not directly resisted by the panels. Afterwards, the PU foam panels exhibits a relatively liner behavior up to about 0.77 atm. In addition, the seamless panel showed a symmetric curvature under the applied monotonic load. Figure 8 depicts this curvature for longitudinal and transverse direction.

Table 3. Deflection at points A to F for test series 1

S panels L.R. #1	Direction	First Monotonic Test (mm)	Second Monotonic Test (mm)	Third Monotonic Test (mm)	Average (mm)	Standard Deviation	CV%
D	longitudinal	14.2	15.1	16	15.1	0.9	6
A	longitudinal	19.7	20.8	20.7	20.4	0.61	3
E	longitudinal	18.3	17.3	18.1	17.9	0.53	3
F	longitudinal	14.7	16.2	16.2	15.7	0.87	5.5
B	transverse	12.2	13	14	13.1	0.9	6.9
C	transverse	12.9	14.1	13.8	13.6	0.63	4.6

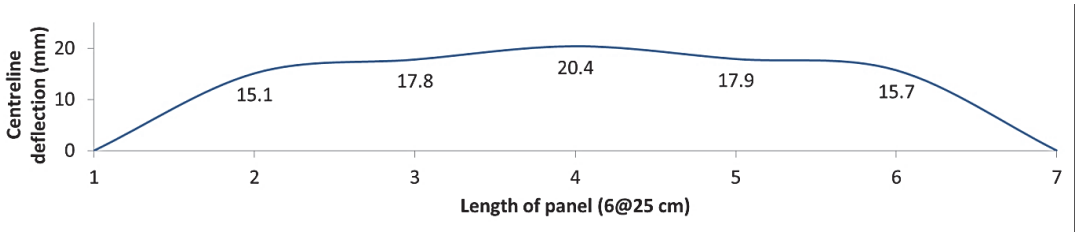

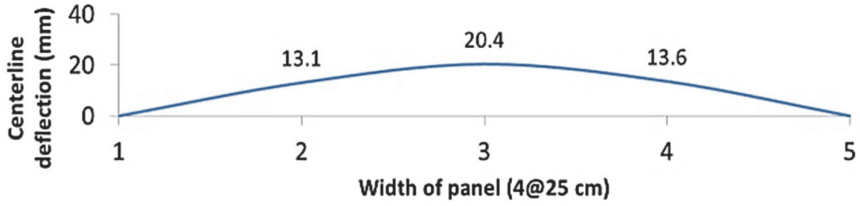

Fig. 8. Symmetric distribution of deflection at the longitudinal and transverse direction in test series 1

A comparison between measured deflections, shown in Fig. 9, point A is at the maximum deflection in all tests.

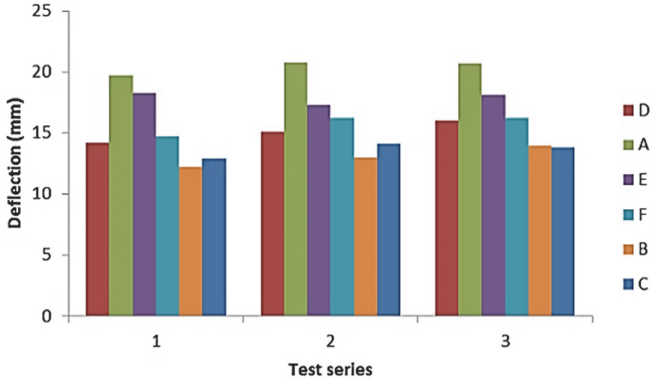

Fig. 9. Comparison between measured deflections (test series 1)

According to these results, the minimum tensile strength of foam can be calculated by Eq. (1), in which $\sigma_{\min,foam}$ is the minimum tensile strength of foam; M is the maximum bending moment (at point A); y is half of the panel thickness (5cm); I is the section's moment of inertia; q is the load equivalent linear intensity; and L is the span (Kaveh & Sharafi, 2007, 2011). Accordingly, this rigid foam panel exhibits a minimum of 13.00 MPa tensile strength.

$$\sigma_{\min,foam} = My / I = qL^2y/(8I) \quad (1)$$

4.2 Test Series 2

In these series of tests, three TS panels were tested under monotonic loading. For all of these panels, similar to test series 1, the maximum deflection appeared at the point A with an average amount of 17.02 mm. Nevertheless, all of these panels collapsed at an average pressure of 0.46 atm at the seam H1 as shown in Figure 10. Therefore, the main mode of collapse is assumed tensile at the seam.

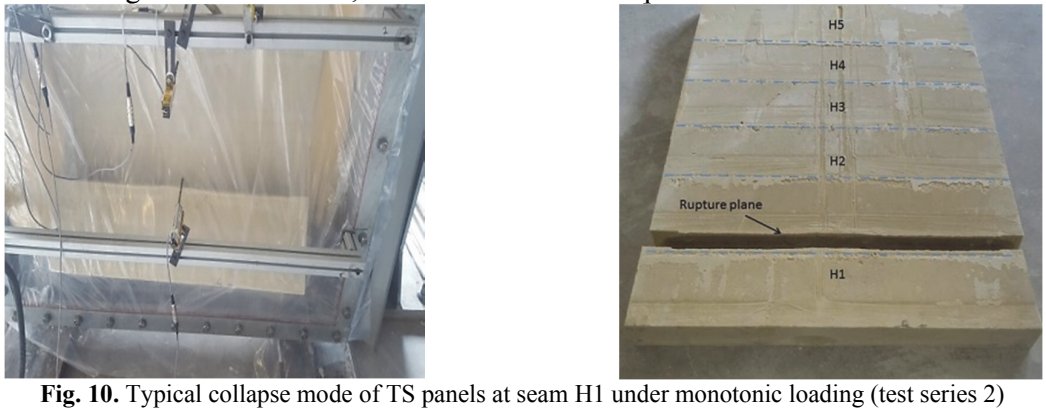

Fig. 10. Typical collapse mode of TS panels at seam H1 under monotonic loading (test series 2)

Similar top the previous case, as shown in Fig. 11, up to about 0.23 atm, the system is at adjusting

phase and exhibits a large primary deflection. Then, TS panels have a semi-liner behaviour before it reaches a pressure of about 0.46 atm. The deflections of pre-identified points of TS panels were measured by potentiometer on the surface. Results shown in Table 4 demonstrate very similar behaviours with those for TS panels under monotonic loading.

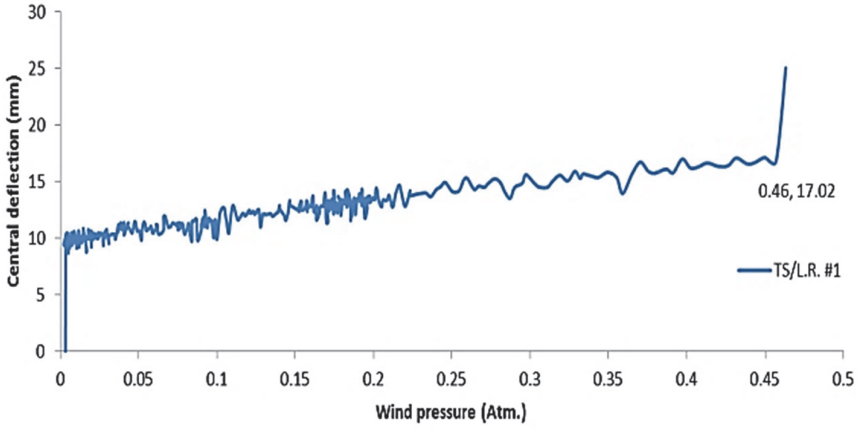

Fig. 11. Wind pressure vs average central deflection in test series 2

Table 4. Deflection at points A to F for test series 2

TS panels L.R. #1	Direction	First Monotonic Test (mm)	Second Monotonic Test (mm)	Third Monotonic Test (mm)	Average (mm)	Standard Deviation	CV%
D	longitudinal	11.8	10.6	11.5	11.3	0.63	5.6
A	longitudinal	16.76	16.9	17.4	17.02	0.34	2
E	longitudinal	15.5	13.6	14.4	14.5	0.95	6.6
F	longitudinal	10.6	12.2	12.3	11.7	0.95	8.1
B	transverse	8	9.6	9.1	8.9	0.82	9.2
C	transverse	7.7	9.1	9.3	8.7	0.87	10

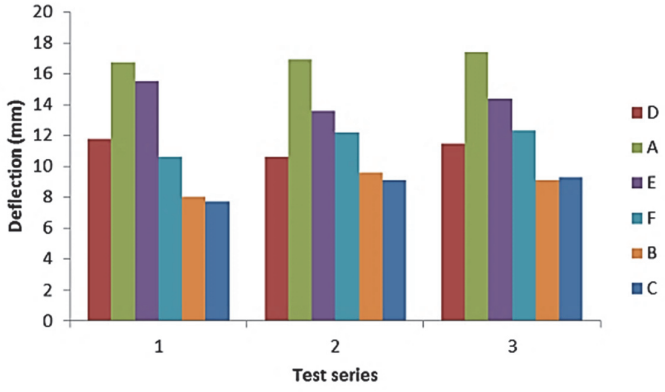

Fig. 12. Comparison between measured deflections of points A to F (test series 2)

Fig. 12 shows a comparison between the measured deflections. Based on the results, in all of the tests, point A (the intersection of centrelines) shows the maximum deflection. In addition, as depicted in Fig. 13 the TS panels exhibit symmetric curvature under monotonic loading in both directions. Fig. 14 illustrates the model used for the analytical analysis of test series 2. The maximum tensile strength of seams under monotonic loading, therefore is calculated by Eq. (2), in which σ_{max} is the maximum tensile strength of the seams. Other parameters are the same as those for Eq (1). Accordingly, this rigid foam panel exhibits a maximum of 4.3 MPa tensile strength.

$$\sigma_{\max,seam} = My / I = \text{qxy(L-x)/(2I)} \quad (2)$$

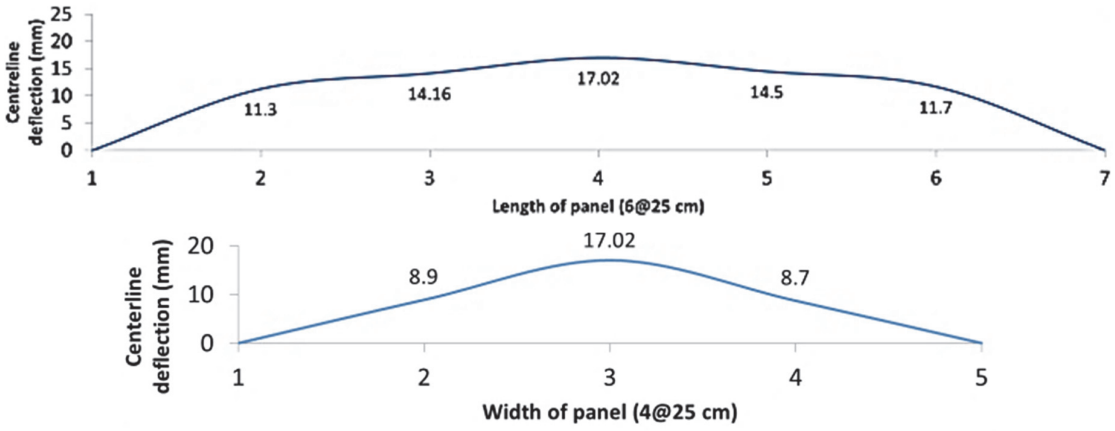

Fig. 13. Distribution of deflection in longitudinal and transverse direction in test series 2

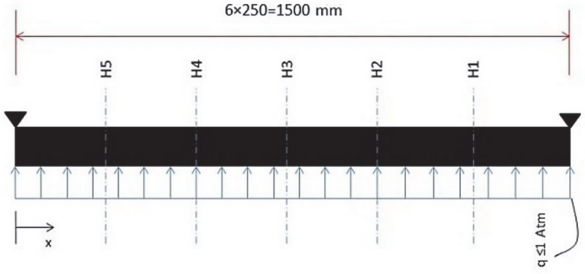

Fig. 14. Analytical model of test series 2

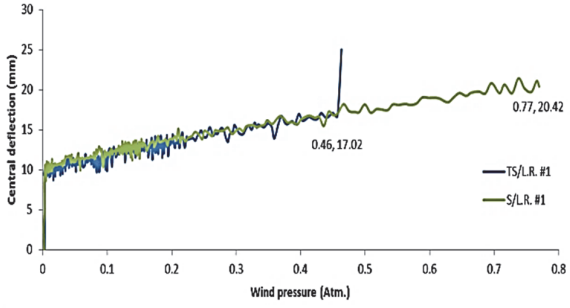

Fig15. Comparison between bending behaviour of S and TS panels under monotonic loading

A comparison between results from Figs. 7 and 11 shows that under monotonic loading, the seamless panels have a larger deflection capacity of about 20% compared to the TS panels (Fig. 15).

4.3 Test Series 3

Three TS panels were tested under cyclic loading, where the results showed all the panels resisted up to a maximum pressure of about 0.33 atm. The deflections of points A to F have been measured by electrical automatic potentiometers, as shown in Table 5. All three panels collapsed at the seam H1 under an average deflection of 8.9 mm. Fig. 16 shows a comparison between the deflections of points A to F. The minimum deflection occurred at Point F, while the maximum deflection of longitudinal centreline of the panel appeared at point A with an average amount of 17.02 mm. It can be seen that the tensile weakness of the seam is the main reason of failure.

Table 5. Deflection at points A to F for test series 3

TS panels L.R. #2	Direction	First cyclic Test (mm)	Second cyclic Test (mm)	Third cyclic Test (mm)	Average (mm)	Standard Deviation	CV%
D	longitudinal	9.9	9.1	9.8	9.6	0.44	4.6
A	longitudinal	11.5	11.4	11.6	11.5	0.1	0.9
E	longitudinal	9.7	9.8	10.2	9.9	0.27	2.7
F	longitudinal	9.4	8.6	8.7	8.9	0.44	4.9
B	transverse	14.1	13.4	13.6	13.7	0.36	2.6
C	transverse	13.8	14.1	13.8	13.9	0.17	1.2

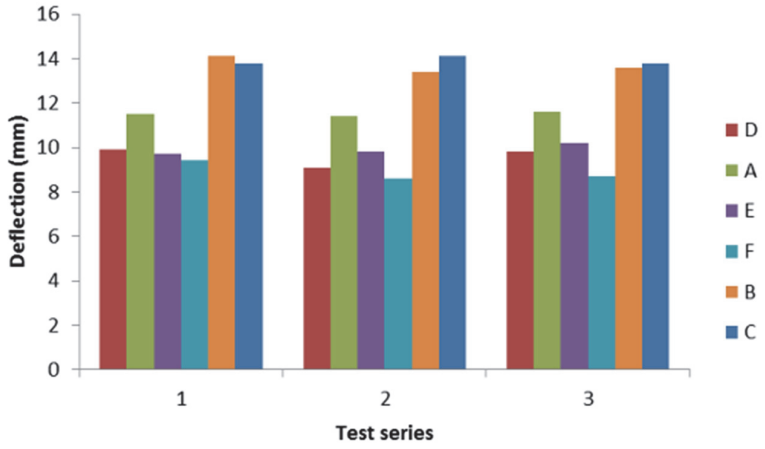

Fig. 16. Comparison between deflections of points A to F in test series 3

Fig. 17 depicts the symmetric distribution of deflection at the longitudinal and transverse centrelines of TS panels. In addition, deflections of the transverse distortion can be seen in this Figure 18. Using Eq. (2), the maximum tensile strength of seams under cyclic loading is calculated as 3.1 MPa.

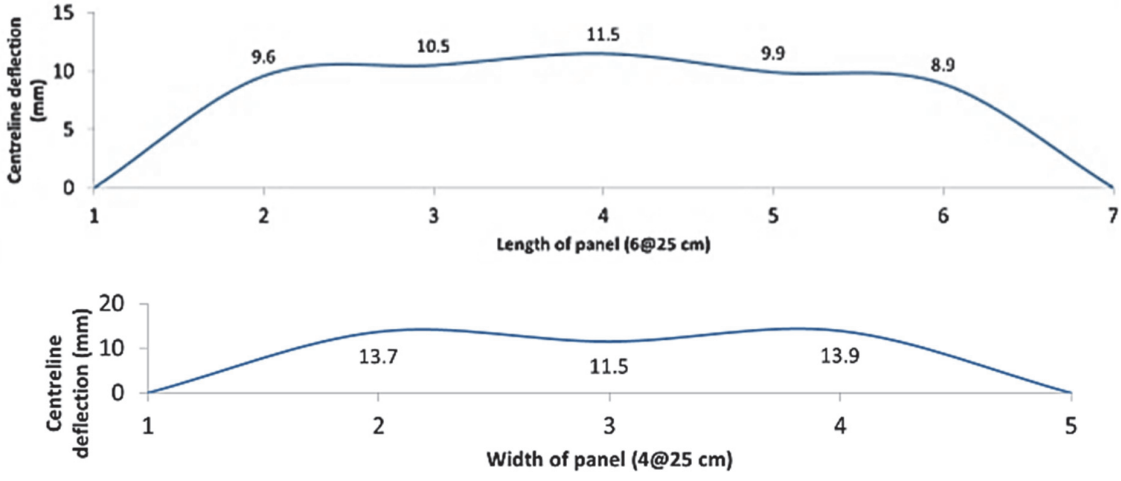

Fig. 17. Distribution of deflection at length (top) and width (down) of panels in test series 3

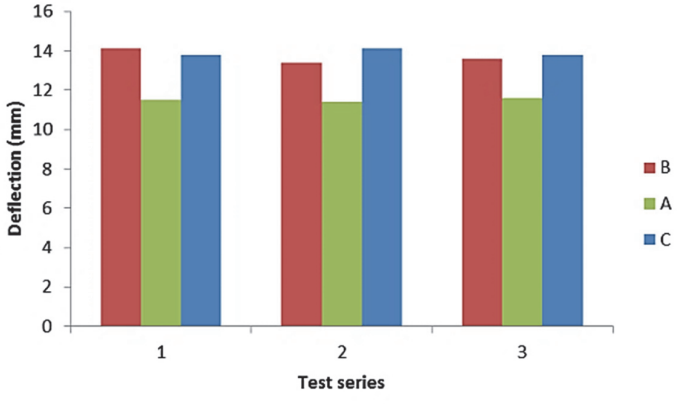

Fig. 18. Comparison between deflections of transverse points A to C for test series 3

4.4 Hysteresis Behaviour

Fig. 19 shows the applied pressure vs max deflection of points A, B and C in the test series 3. Based on these figures, point A has the most regular and narrowest hysteresis diagram, with the minimum capacity for energy absorption. However, points B and C showed better and relatively more similar hysteresis behaviour that demonstrates that the TS panels exhibit rather symmetric hysteresis behaviour in transverse direction under cyclic loads.

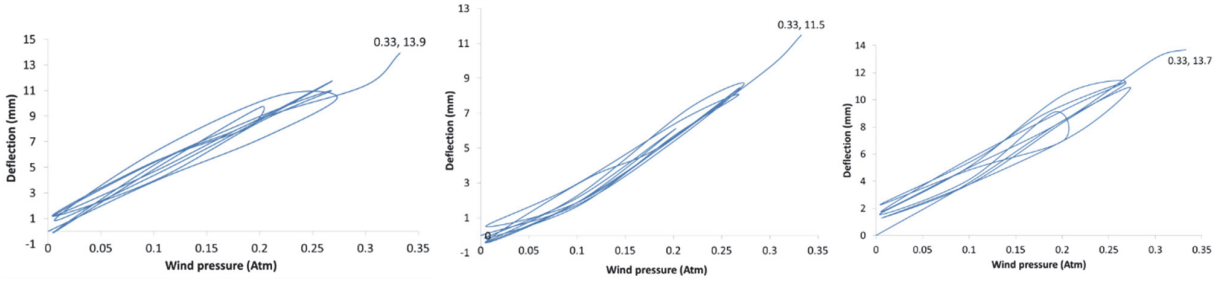

Fig. 19. Applied pressure vs deflection of point B, A and C in test series 3 (left to right) in test series 3

The applied cyclic pressure vs max deflection of points D, A and F in the test series 3 are shown in Figure 20. It reveals that points D and F exhibit two different hysteresis behaviours: Point D has a relative wide and irregular hysteresis diagram in comparison with the point F. The different internal structure of seams at these points can be assumed as the main reason of such difference.

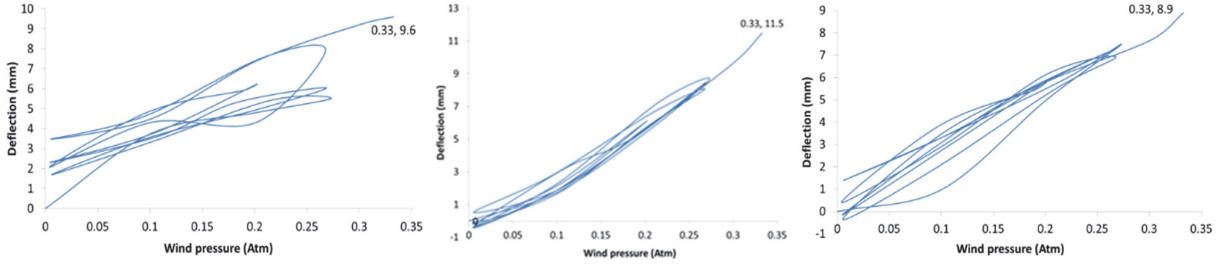

Fig. 20. Applied pressure vs deflection of points D (left), A (middle) and F (right) in test series 3

The deflection time history of points A to F in test series 3 are shown in Figs. 21 and 22. The relative areas of these graphs addressing the relative energy absorption capacity of seams H1 to H5 under cyclic loading are calculated and presented in Table 6.

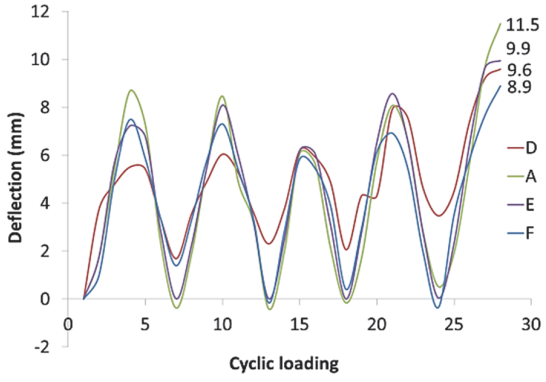

Fig. 21. Deflection time history for longitudinal centreline in the test series 3

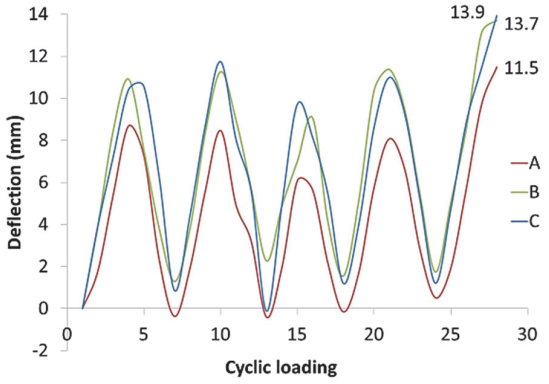

Fig. 22. Deflection time history for transverse centreline in the test series 3

Table 6. Comparison between relative absorbed energy at seams H1 to H5 under cyclic loading.

Seam	H1	H2	H3	H4	H5
Relative absorbed energy	1	1.02	1.53	1.02	1.21

Comparison between Table 6 and Fig. 5 indicates that making the seams at end of the gel time (H3) can increase the energy absorption capacity by 53%, compared to the end of take free time (H1).

5. Concluding remarks

A comparison between the results of the monotonic tests shows that:

- ✓ Casting at the end of gel time instead the end of tack free time, resulted in an %80 increase in the tensile strength of the seams ($[X_{H1}(L-X_{H1})] / [X_{H3}(L-X_{H3})]$).
- ✓ Casting at about 20 sec before of the end of tack free time (120^{th} sec), increased the tensile strength of the seams by %60 ($[X_{H1}(L-X_{H1})] / [X_{H4}(L-X_{H4})]$).
- ✓ The seamed section exhibited about 33.1% of the maximum tensile strength of an intact section.
- ✓ Under monotonic loading, the seamless panels showed a larger deflection capacity, as 20% more than that of TS panels.

A comparison between the results of the cyclic tests shows that:

- ✓ Casting at the end of tack free time (120^{th} sec) instead of 110^{th} sec resulted in a significant positive effect on the tensile strength of seams.
- ✓ The tensile strength of a seamed section was under cyclic loading about 72.1% of the strength under monotonic loading.
- ✓ Making the seams at the end of the gel time increased the energy absorption capacity of panels by 53% in comparison with the end of take free time.

References

ASTM-E1730 (2015). Standard Specification for Rigid Foam for Use in Structural Sandwich Panel Core. ASTM International. West Conshohocken, PA.

Aliha, M. R. M., Linul, E., Bahmani, A., & Marsavina, L. (2018a). Experimental and theoretical fracture toughness investigation of PUR foams under mixed mode I+ III loading. *Polymer Testing*, *67*, 75-83.

Aliha, M. R. M., Bahmani, A., Linul, E., Marsavina, L., Mousavi S.S., & Mousavi A. (2018b). Investigation of fracture initiation angle and propagation path for PUR foams under mixed mode

I/III loading. In: Proceedings of the 6th international conference on crack path September 2018, Verona, Italy.

Defonseka, C. (2013). *Practical guide to flexible polyurethane foams*. Smithers Rapra.

Fan, X., Zhao, M., & Wang, T. (2017). Experimental investigation of the fatigue crack propagation in a closed-cell aluminum alloy foam. *Materials Science and Engineering: A*, *708*, 424-431.

Huang, J. S., & Lin, J. Y. (1996). Fatigue of cellular materials. *Acta materialia*, *44*(1), 289-296.

Kanny, K., Mahfuz, H., Carlsson, L. A., Thomas, T., & Jeelani, S. (2002). Dynamic mechanical analyses and flexural fatigue of PVC foams. *Composite Structures*, *58*(2), 175-183.

Kaveh, A., & Sharafi, P. (2007). A simple ant algorithm for profile optimization of sparse matrices. *Asian Journal of Civil Engineering (Building and Housing)*, *9*(1), 35-46.

Kaveh, A., & Sharafi, P. (2011). Charged system search algorithm for minimax and minisum facility layout problems. *Asian Journal of Civil Engineering*, *12*(6), 703-718.

Marsavina, L., Linul, E., Voiconi, T., & Sadowski, T. (2013). A comparison between dynamic and static fracture toughness of polyurethane foams. *Polymer Testing*, *32*(4), 673-680.

Nemati, S., Sharafi, P., Samali, B., Aliabadizadeh, Y., & Saadati, S. (2018). Non-reinforced foam filled modules for rapidly assembled post disaster housing. *International Journal of GEOMATE*, *14*(45), 151-161.

Noble, F. W., & Lilley, J. (1981). Fatigue crack growth in polyurethane foam. *Journal of Materials Science*, *16*(7), 1801-1808.

Poapongsakorn, P., & Kanchanomai, C. (2013). Fatigue crack growth behavior and mechanism of closed-cell PVC foam. *Polymer Engineering & Science*, *53*(8), 1719-1727.

Sharafi, P., Nemati, S., Samali, B., Bahmani, A., & Khakpour, S. (2018 a). Behavior of integrated connections between adjacent foam-filled modular sandwich panels. *Engineering Solid Mechanics*, *6*(4), 361-370.

Sharafi, P., Nemati, S., Samali, B., Bahmani, A., Khakpour, S., & Aliabadizadeh, Y. (2018 b). Flexural and shear performance of an innovative foam-filled sandwich panel with 3-D high density polyethylene skins. *Engineering Solid Mechanics*, *6*(2), 113-128.

Sharafi, P., Samali, B., Ronagh, H., & Ghodrat, M. (2017). Automated spatial design of multi-story modular buildings using a unified matrix method. *Automation in Construction*, *82*, 31-42.

Shipsha, A., Burman, M., & Zenkert, D. (2000). On mode I fatigue crack growth in foam core materials for sandwich structures. *Journal of Sandwich Structures & Materials*, *2*(2), 103-116.

Toubia, E. A., & Elmushyakhi, A. (2017). Influence of core joints in sandwich composites under in-plane static and fatigue loads. *Materials & Design*, *131*, 102-111.

Wang, L., Limodin, N., El Bartali, A., Witz, J. F., Seghir, R., Buffiere, J. Y., & Charkaluk, E. (2016). Influence of pores on crack initiation in monotonic tensile and cyclic loadings in lost foam casting A319 alloy by using 3D in-situ analysis. *Materials Science and Engineering: A*, *673*, 362-372.

Zenkert, D., & Burman, M. (2009). Tension, compression and shear fatigue of a closed cell polymer foam. *Composites Science and Technology*, *69*(6), 785-792.

Zhao, M. D., Fan, X., Fang, Q. Z., & Wang, T. J. (2015). Experimental investigation of the fatigue of closed-cell aluminum alloy foam. *Materials Letters*, *160*, 68-71.